Park and Chang *Molecular Brain* (2018) 11:10
https://doi.org/10.1186/s13041-018-0353-z

Molecular Brain

SHORT REPORT Open Access

Soluble $A\beta_{1-42}$ increases the heterogeneity in synaptic vesicle pool size among synapses by suppressing intersynaptic vesicle sharing

Daehun Park[1] and Sunghoe Chang[1,2*]

Abstract

Growing evidence has indicated that prefibrillar form of soluble amyloid beta ($sA\beta_{1-42}$) is the major causative factor in the synaptic dysfunction associated with AD. The molecular changes leading to presynaptic dysfunction caused by $sA\beta_{1-42}$, however, still remains elusive. Recently, we found that $sA\beta_{1-42}$ inhibits chemically induced long-term potentiation-induced synaptogenesis by suppressing the intersynaptic vesicle trafficking through calcium (Ca^{2+}) dependent hyperphosphorylation of synapsin and CaMKIV. However, it is still unclear how $sA\beta_{1-42}$ increases intracellular Ca^{2+} that induces hyperphosphorylation of CaMKIV and synapsin, and what is the functional consequences of $sA\beta_{1-42}$-induced defects in intersynaptic vesicle trafficking in physiological conditions. In this study, we showed that $sA\beta_{1-42}$elevated intracellular Ca^{2+} through not only extracellular Ca^{2+} influx but also Ca^{2+} release from mitochondria. Surprisingly, without Ca^{2+} release from mitochondria, $sA\beta_{1-42}$ failed to increase intracellular Ca^{2+} even in the presence of normal extracellular Ca^{2+}. We further found that $sA\beta_{1-42}$-induced mitochondria Ca^{2+} release alone sufficiently increased Serine 9 phosphorylation of synapsin. By blocking synaptic vesicle reallocation, $sA\beta_{1-42}$ significantly increased heterogeneity of total synaptic vesicle pool size among synapses. Together, our results suggested that by disrupting the axonal vesicle trafficking, $sA\beta_{1-42}$ disabled neurons to adjust synaptic pool sizes among synapses, which might prevent homeostatic rescaling in synaptic strength of individual neurons.

Background

Abnormal synaptic function is one of the earliest known defects in Alzheimer's disease (AD) [1]. Recent studies have indicated that the non-fibrillar soluble oligomeric form of amyloid β protein (sAβ) rather than insoluble amyloid fibrils or plaques [2–4] is the cause of the synaptic dysfunction and cognitive defects associated with AD. Indeed, biochemical analysis of postmortem AD tissue has revealed a robust correlation between sAβ levels and the extent of synapse loss and cognitive impairment [2]. The accumulation of sAβ also closely correlates with cognitive decline in animal models and AD patients and is primarily due to disrupting synaptic plasticity [5], Ca^{2+} homeostasis [6–8] and signaling pathways such as glycogen synthase kinase 3 beta (GSK-3β) [9], c-Jun [10], Ca^{2+}/calmodulin-dependent protein kinase kinase (CaMKK), AMP-activated protein kinase (AMPK) [11], cytoskeletal networks [12] and axonal transport [13]. The 42-residue amyloid beta protein ($sA\beta_{1-42}$) has been shown to impair long-term potentiation (LTP), and to be neurotoxic [14]. A number of different postsynaptic mechanisms, including dendritic spine loss, alteration of 2-amino-3-(5-methyl-3-oxo-1,2-oxazol-4-yl) propanoic acid (AMPA) and N-methyl-D-aspartic acid (NMDA) receptor numbers have been implicated in $sA\beta_{1-42}$-induced synaptic dysfunction [15–17] while the molecular changes leading to presynaptic dysfunction by $sA\beta_{1-42}$ have not been clearly identified [18–23].

Previous studies have showed that axonal synaptic vesicles diffuse laterally along the axon and trading of synaptic vesicles (SVs) between synapses reallocates

* Correspondence: sunghoe@snu.ac.kr
[1]Department of Physiology and Biomedical Sciences, Seoul National University College of Medicine, Seoul 03080, South Korea
[2]Neuroscience Research Institute, Medical Research Center, Seoul National University College of Medicine, Seoul 03080, South Korea

functional SV pools and synaptic strength, leading to dynamically regulate presynaptic properties [24–26]. One of physiological consequences of intersynaptic vesicle sharing includes a rapid new functional synapse formation upon synaptic plasticity [26, 27]. Recently, we have found that $sA\beta_{1-42}$ inhibits chemical LTP (cLTP)-induced synaptogenesis by suppressing the intersynaptic vesicle trafficking. We further found that $sA\beta_{1-42}$ rapidly increases intracellular Ca^{2+}, which causes hyperphosphorylation of synapsin and CaMKIV and this is a key pathway responsible for the inhibitory effect of $sA\beta_{1-42}$ on the regulation of intersynaptic vesicle trafficking [27]. We, however, do not know how $sA\beta_{1-42}$ increases intracellular Ca^{2+} which is critical for the phosphorylation-dependent dissociation of synapsin-SV-actin ternary complex [27]. The sharing between the SV pools over synapse also contributes to resizing of the SV pool at a single synapse, leading to homeostatic changes in synaptic pool sizes in neurons [26]. Since $sA\beta_{1-42}$-suppresses intersynaptic vesicle trafficking, it could affect homeostatic regulation of SV pool size, which is currently unknown.

In this study, we have addressed these two important issues. We found that $sA\beta_{1-42}$ rapidly elevated intracellular Ca^{2+} through not only extracellular Ca^{2+} influx but also Ca^{2+} release from mitochondria. Surprisingly, $sA\beta_{1-42}$ induced Ca^{2+} release from mitochondria is critical for extracellular Ca^{2+} influx, and it also sufficiently hyperphosphorylates synapsin which is important for intersynaptic vesicle trafficking. We also showed that acute treatment of $sA\beta_{1-42}$ to cultured rat hippocampal neurons strongly blocked SV reallocation, leading to a significant increase in heterogeneity in SV pool size among synapses.

Results

$sA\beta_{1-42}$-induced Ca^{2+} release from mitochondria is critical for extracellular Ca^{2+} influx

Our previous study have found that acute treatment (2 h) of $sA\beta_{1-42}$ greatly increases the presynaptic Ca^{2+} level, which leads to hyperphosphorylation of CaMKIV (T196) and synapsin (S9) [27] (also confirmed in Fig. 1a). Ca^{2+} and CaMKIV mediated phosphorylation of synapsin S9 dissociates SV-synapsin-actin ternary complex and this is a critical pathway for $sA\beta_{1-42}$ effect to inhibit intersynaptic vesicle trafficking [27]. However, the source of cytosolic Ca^{2+} upraised by $sA\beta_{1-42}$ treatment has remained unknown. To solve this question, we loaded neurons with Fluo-4 AM to monitor changes in cytosolic Ca^{2+} levels (Fig. 1b). $sA\beta_{1-42}$ markedly increased intracellular Ca^{2+} after 5 min treatment in 2 mM extracellular Ca^{2+} concentration (Fig. 1b). Similar to this result, phosphorylation of synapsin was also increased after $sA\beta_{1-42}$ treatment (Fig. 1c). The amount of phosphorylated synapsin by $sA\beta_{1-42}$ was not affected by treatment time (3 min to 6 h) (Fig. 1c). Next, we measured $sA\beta_{1-42}$-induced cytosolic Ca^{2+} elevation in real-time and found that $sA\beta_{1-42}$ rapidly increases intracellular Ca^{2+} right after treatment in 2 mM extracellular Ca^{2+} concentration (Fig. 1d). $sA\beta_{1-42}$, however, also evoked a small but significant rises cytosolic Ca^{2+} even in the absence of extracellular Ca^{2+} (Fig. 1d). These results suggested that $sA\beta_{1-42}$ increased the cytosolic Ca^{2+} level by mainly inducing extracellular Ca^{2+} influx but partially stimulating the other intracellular Ca^{2+} stores. Mitochondria have been known to act as important internal Ca^{2+} source and to be dysregulated in Alzheimer's disease [28]. To test the effects of $sA\beta_{1-42}$ on mitochondria Ca^{2+} release, we blocked mitochondrial Ca^{2+} efflux by applying tetraphenylphosphonium (TPP), which blocks Ca^{2+} efflux from mitochondria [29]. TPP completely eliminated $sA\beta_{1-42}$-induced rise in Ca^{2+}signal in the absence of extracellular Ca^{2+} (Fig. 1d). Surprisingly, when mitochondria Ca^{2+} efflux was blocked by TPP, cytosolic Ca^{2+} increment by $sA\beta_{1-42}$ was significantly decreased despite the presence of 2 mM extracellular Ca^{2+} (Fig. 1d). Furthermore, when we pretreated carbonyl cyanide p-(trifluoromethoxy)-phenylhydrazone (FCCP) to deplete the mitochondria Ca^{2+} and then treated with $sA\beta_{1-42}$ (Fig. 1e), the increment of cytosolic Ca^{2+} by $sA\beta_{1-42}$ was not observed even in the presence of extracellular Ca^{2+} (Fig. 1e).

Next we tested whether mitochondrial Ca^{2+} release by $sA\beta_{1-42}$ is sufficient to phosphorylate synapsin. We found that phosphorylation of synapsin was signicantly increased by $sA\beta_{1-42}$-induced mitochondrial Ca^{2+}release (without extracellular Ca^{2+}) and restored by TPP treatment (Fig. 1f). These results indicated that $sA\beta_{1-42}$-evoked rise in cytosolic Ca^{2+} was mostly due to the Ca^{2+} coming from outside of the cells, but the release of Ca^{2+} from the mitochondria plays an important role to induce extracellular Ca^{2+} influx and could phosphorylates synapsin.

$sA\beta_{1-42}$ inhibits intersynaptic movements of synaptic vesicle and synapsin

Since phosphorylation of synapsin is a key mechanism for $sA\beta_{1-42}$-induced defect in the intersynaptic vesicle trafficking, the overexpression of phospho-deficient mutant of synapsin Ia completely restore the $sA\beta_{1-42}$-induced inhibition of intersynaptic vesicle movements [27]. Accordingly, we further found that phospho-deficient mutant (S9A) of synapsin Ia had much higher binding affinity for actin, which is important for maintaining intersynaptic trafficking (Additional file 1: Figure S1). In addition, we confirmed that $sA\beta_{1-42}$ strongly suppressed intersynaptic vesicle trafficking as previously described (Fig. 2a-c) [27].

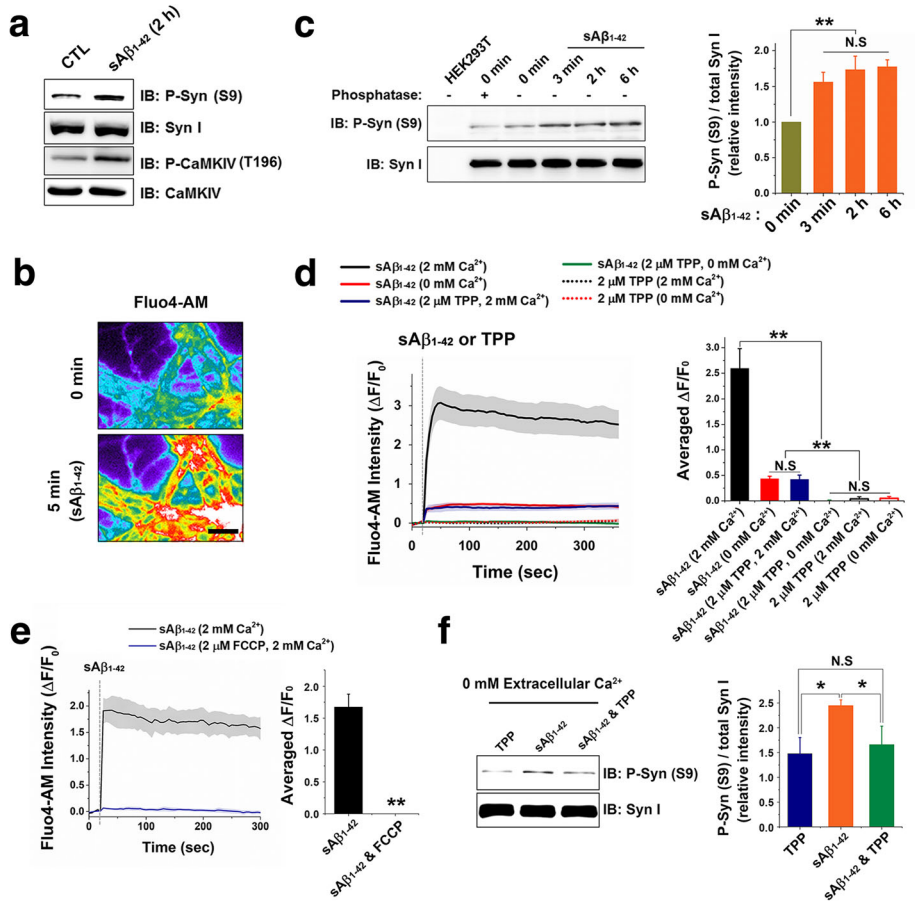

Fig. 1 $sA\beta_{1-42}$ increases cytosolic Ca^{2+} concentration by inducing mitochondria Ca^{2+} release dependent extracellular Ca^{2+} influx. **a** Cultured neurons were pretreated as indicated and analyzed for the level of each phospho-synapsin (S9) and phospho-CaMKIV (T196). **b** Representative images for Fluo-4 AM after treatment with 200 nM $sA\beta_{1-42}$ for 5 min (Scale bar = 5 μm). **c** Neurons were treated with $sA\beta_{1-42}$ for the time as indicated and phosphorylation of synapsin was measured by the western blot (1 ± 0 for 0 min, 1.56 ± 0.13 for 3 min, 1.73 ± 0.19 for 2 h, 1.77 ± 0.10 for 6 h $sA\beta_{1-42}$ treatment, $n = 4$ independent blots). Equal amount of HEK293T cell lysates and neuron lysates incubated with phosphatase were loaded to confirm the synapsin and phospho-synapsin bands. **d** Fluo-4 AM intensity plots after treatment with 200 nM $sA\beta_{1-42}$ or 2 μM TPP in the indicated extracellular buffer (in brackets). Averaged $\Delta F/F_0$ was calculated by averaging the last 20 points of fluorescence profiles (2.59 ± 0.39 for $sA\beta_{1-42}$ in 2 mM extracellular Ca^{2+}, 0.43 ± 0.05 for $sA\beta_{1-42}$ in 0 mM extracellular Ca^{2+}, 0.42 ± 0.08 for $sA\beta_{1-42}$ in 2 mM extracellular Ca^{2+} with TPP, 0.00 ± 0.01 for $sA\beta_{1-42}$ in 0 mM extracellular Ca^{2+} with TPP, 0.04 ± 0.04 for TPP in 2 mM extracellular Ca^{2+}, 0.05 ± 0.03 for TPP in 0 mM extracellular Ca^{2+} ($n \geq 5$ independent experiments for each group)). **e** Fluo-4 AM loaded neurons were pretreated as indicated (in brackets) for 5 min and treated with 200 nM $sA\beta_{1-42}$ (Averaged $\Delta F/F_0$: 1.67 ± 0.20 for $sA\beta_{1-42}$ ($n = 3$ independent experiments), 0.00 ± 0.03 for $sA\beta_{1-42}$ with FCCP ($n = 4$ independent experiments)). **f** Neurons were treated with the indicated medium for 2 h and their phospho-synapsin (S9) and total synapsin level were detected by western blot and analyzed (Phospho-synapsin/total-synapsin: 1 ± 0 for control, 1.48 ± 0.32 for control with TPP, 2.45 ± 0.11 for $sA\beta_{1-42}$, 1.66 ± 0.37 for $sA\beta_{1-42}$ with TPP, $n = 3$ independent blots). Values are means ± standard error of mean (SEM). N.S = no significant difference, * $p < 0.05$, ** $p < 0.01$ (ANOVA and Tukey's HSD post hoc test for (**c**, **d**, **f**) and Student's *t*-test for (**e**))

Previous study showed that synapsin itself laterally moves between neighboring synapses [30]. Thus, we examine the dynamic behavior of synapsin in response to $sA\beta_{1-42}$ using a fluorescence recovery after photobleaching (FRAP) and analyzed whether $sA\beta_{1-42}$ affects the movement of synapsin as well. We transfected GFP-synapsin into neurons, and then selectively photo-bleached a single presynapse and monitored the recovery of fluorescence (Fig. 2d). After photo-bleaching, substantial recovery of GFP-synapsin fluorescence (~ 70%) was observed in the control neurons (Fig. 2d, e). However, in boutons treated with $sA\beta_{1-42}$, fluorescence recovery occurred less and slower than in the control group (Fig. 2d-g). Preincubation of $sA\beta_{1-42}$ with 6E10 antibody completely blocked the $sA\beta_{1-42}$ effect (Fig. 2d-g). These data strongly suggested that $sA\beta_{1-42}$ suppressed the intersynaptic movements of both SVs and synapsin.

$sA\beta_{1-42}$ significantly increases heterogeneity of total SV pools among synapses

Since the lateral trafficking and sharing of SVs among synapses have been known to regulate presynaptic

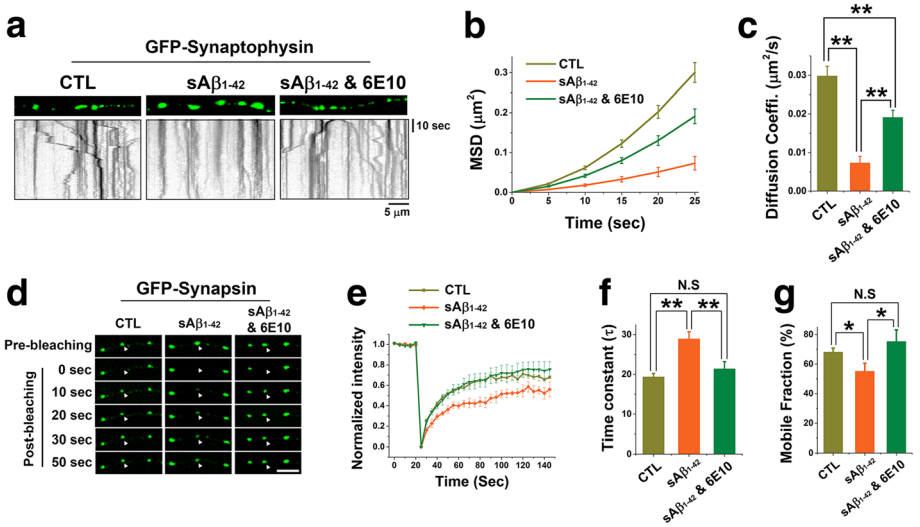

Fig. 2 $sA\beta_{1-42}$ suppressed the intersynaptic vesicle movement and synapsin. **a-c** Neurons expressing GFP-synaptophysin were treated as indicated and imaged for 1 min to track the intersynaptic vesicles. **a** Representative kymographs showing trafficking of GFP-synaptophysin in each group. **b** MSD curves versus time. **c** Diffusion coefficients, $n = 7$ independent experiments for each group. **d-g** Neurons were transfected with GFP-synapsin (DIV8) and treated as indicated at DIV14. A single bouton was selectively photobleached and its recovery time was measured through FRAP assay. **d** Representative time-lapse images of FRAP assay for control, $sA\beta_{1-42}$ and $sA\beta_{1-42}$ with 6E10 (scale bar = 5 μm). White arrowheads indicate bleached boutons. **e** Average plots of fluorescence intensities (normalized to initial intensities) before and after photobleaching. **f** Fluorescence recovery traces in (**e**) were fitted to a single exponential function with time constant (τ) of 19.36±0.84 s for control, 28.92±1.8 s for $sA\beta_{1-42}$, and 21.38±1.82 s for $sA\beta_{1-42}$ with 6E10, respectively ($n = 4$ independent experiments for each group). **g** Mobile fractions were calculated by averaging final 5 values in (**e**). Mobile fraction (%): 68.10±2.67 for control, 55.13±5.47 for $sA\beta_{1-42}$, and 75.25±7.85 for $sA\beta_{1-42}$ with 6E10 ($n = 4$ independent experiments for each group). Values are means±SEM. N.S = no significant difference, * $p < 0.05$, ** $p < 0.01$ (ANOVA and Tukey's HSD post hoc test))

properties by reallocating SVs and thus balancing the SV pool size among synaptic neighbors [24, 26, 31], we suspected that the defects in lateral intersynaptic trafficking of SV by $sA\beta_{1-42}$ could affect homeostatic regulation of SV pool size among synapses.

We first stained neurons with the synaptic vesicle marker, synaptophysin and the active zone marker, bassoon after treatment with or without $sA\beta_{1-42}$ to check if there are any morphological changes in presynaptic terminals. When we stained neurons with synaptophysin antibody to measure total synaptic vesicle pool size [32–34], we found that $sA\beta_{1-42}$ treated neurons showed higher variability of the size of presynaptic boutons than the control group, while they showed the similar number of presynaptic boutons with the control group (Fig. 3a, b). The intensity of bassoon, a presynaptic active zone marker, however, was not different between $sA\beta_{1-42}$ treated and untreated neurons (Fig. 3c), demonstrating that $sA\beta_{1-42}$ treatment increased heterogeneity of total SV pool size without altering the morphology of presynaptic terminals.

To confirm that this did not come from a biased undersampling, we plotted the pooled distribution histogram of synaptophysin intensities obtained from over 80,000 individual boutons. We found that $sA\beta_{1-42}$ increased the mean value of the total SV pool size (Fig. 3d, e). More importantly, when the distribution of bouton intensities was fitted to a gamma function with a fixed-shape parameter ($\alpha = 4$), the scale parameter (β), which indicates the degree of dispersion of the distribution, was significantly larger in neurons exposed to $sA\beta_{1-42}$ than in the control or $sA\beta_{1-42}$-6E10 treated group (Fig. 3d, e). These results indicate that $sA\beta_{1-42}$ significantly increases heterogeneity between presynapses and thus affects homeostatic rescaling by inhibiting intersynaptic vesicle trafficking.

Discussion

Substantial data have indicated that $sA\beta_{1-42}$ causes the synaptic dysfunction observed in AD [3]. $sA\beta_{1-42}$ alters synaptic plasticity by inhibiting long-term potentiation and facilitating long-term depression [35, 36]. These changes induce the loss of dendritic spines, modulate the expression of AMPA and NMDA receptors and interfere with Ca^{2+} homeostasis [4, 15, 17, 37]. Much less attention, however, has been paid to the effect of $sA\beta_{1-42}$ on the presynaptic function. Moreover, there have been highly contradictory observations about the effects of $sA\beta_{1-42}$ on presynapses depending on its source [18, 20] or concentration [18, 22]. Here, we found that $sA\beta_{1-42}$ induces mitochondrial Ca^{2+} release and it is critical for extracellular Ca^{2+} influx across the plasma membrane and hyperphosphorylation of synapsin. We also have figured out that $sA\beta_{1-42}$ strongly increases heterogeneiety of presynaptic vesicle pool sizes by

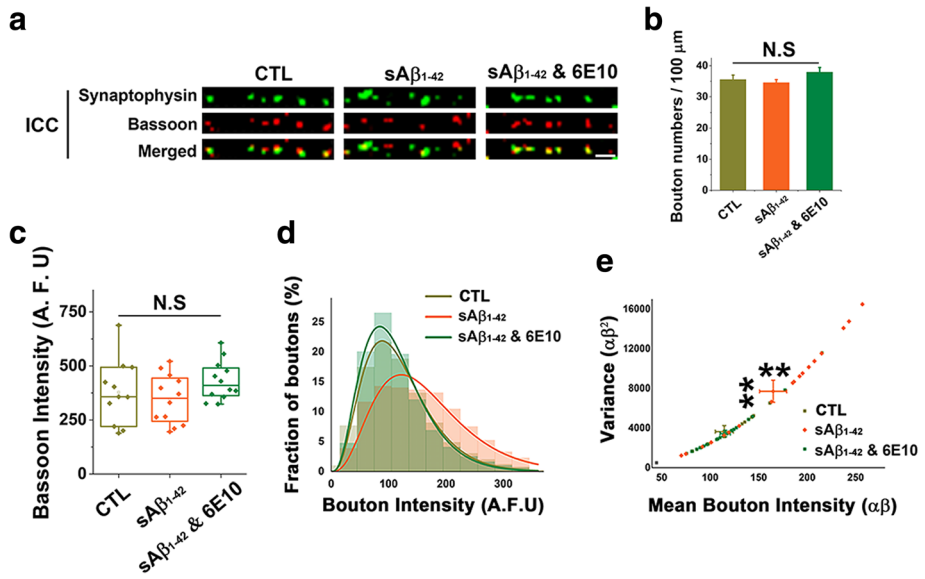

Fig. 3 $sA\beta_{1-42}$ increases heterogeneity of presynaptic terminals. **a-e** Neurons were treated as indicated and immunostained for endogenous synaptophysin and bassoon. **a** Representative immunocytochemistry images (scale bar = 2 μm). **b** The number of presynaptic boutons were counted along the axon (Average bouton numbers per 100 μm axon length: 35.54±1.43 for control, 34.57±0.97 for $sA\beta_{1-42}$, and 37.92±1.53 for $sA\beta_{1-42}$ with 6E10 ($n = 4$ independent experiments for each group)). **c** The intensity of bassoon puncta (> 80,000) was measured and presented with the box plot. **d** The intensity profiles of synaptophysin-stained boutons were fitted into gamma distribution with a fixed shape parameter α = 4. The scale parameter β was as follows: Control = 29.56 (81,356 boutons); $sA\beta_{1-42}$ = 40.70 (89,599 boutons); $sA\beta_{1-42}$ with 6E10 = 28.20 (83,369 boutons). **e** Raw data of (d) were fitted to gamma function and their mean bouton intensity (α x β) and variance (α x β^2) were measured. Values are means±SEM. N.S = no significant difference, ** $p < 0.01$ (ANOVA and Tukey's HSD post hoc test)

disrupting SV pool sharing which is affected by synapsin phosphorylation.

We also have found that $sA\beta_{1-42}$-mediated Ca^{2+} increment is the major causative factor in the presynaptic dysfunction associated with intersynaptic vesicle trafficking [27]. However, we have not revealed the Ca^{2+} sources involved in this phenomenon [27]. Although the precise mechanism is still elusive, previous studies have suggested that $sA\beta_{1-42}$ trigger not only internal Ca^{2+}release from endoplasmic reticulum (ER) [38] but also extracellular Ca^{2+} influx by altering membrane Ca^{2+}permeability, interacting with voltage-gated Ca^{2+}channels or forming Aβ pores, [7, 39]. Here, we found that extracellular Ca^{2+} made up a large portion of the total Ca^{2+} incremented by $sA\beta_{1-42}$ treatment, whereas small but significant portion was constituted by Ca^{2+}released from mitochondria. In addition, mitochondria Ca^{2+} efflux was required for the extracellular Ca^{2+} influx by $sA\beta_{1-42}$. Although the precise molecular mechanism of how released Ca^{2+} from mitochondria induces extracellular Ca^{2+} influx certainly requires further study, we could speculate some possibilities. The released Ca^{2+} from mitochondria by $sA\beta_{1-42}$ could act as a signaling molecule and activates some Ca^{2+} channels in plasma membrane. For example, previous study indicates that mitochondrial Ca^{2+} released by FCCP activates extracellular signal regulated kinase (ERK) 1/2 in PC12 cells [40]. Indeed, ERK phosphorylates α1 and β subunits of N-type VDCCs (voltage-dependent calcium channels) [41] and enhances VDCC current in sensory neurons [42]. Therefore, although the amount of Ca^{2+} released from mitochondria by $sA\beta_{1-42}$ is small, it may play critical role in the early stage of Ca^{2+} signaling. In this study, we also found that $sA\beta_{1-42}$-induced Ca^{2+} release from mitochondria without extracellular Ca^{2+} influx was sufficient to increase S9 phosphorylation of synapsin, indicating that small amount of Ca^{2+} release from mitochondria could sufficiently regulate the intersynaptic vesicle trafficking. However, unlike FCCP, TPP pretreatment did not completely block the $sA\beta_{1-42}$-induced Ca^{2+} influx across the membrane. These discrepancies may be due to the differences in the molecular mechanism of action, side effects of drugs or dose dependent manners. FCCP, a mitochondira proton gradient uncoupler, induces mitochondrial Ca^{2+} release as a proton inophore [43]. On the contrary, TPP specifically blocks both sodium-dependent and independent Ca^{2+} efflux from mitochondria [44]. However, TPP has around 50 times lower inhibitory constant (K_i) value in sodium-dependent pathway than sodium-independent pathway and it means that sodium-dependent Ca^{2+} efflux is efficiently blocked by TPP [44]. In addition, previous study has showed that FCCP induces release of Ca^{2+} from not only mitochondria but also other non-mitochondrial Ca^{2+} sources [45]. Thus, we still cannot completely rule out the other internal Ca^{2+} sources

for $sA\beta_{1-42}$-induced cytosolic Ca^{2+} elevation. Specifically, ER can have a significant role because ER and mitochondria work together to regulate intracellular Ca^{2+} levels [46]. In addition, previous study has shown that $sA\beta_{1-42}$ forms a cation-selective channels on the membrane and Zn^{2+} treatment can block the open pore [47]. Therefore, we tried to test the blockade effect of Zn^{2+} in the $sA\beta_{1-42}$-induced cytosolic Ca^{2+} elevation. However, preincubation of Zn^{2+} largely increased basal Fluo-4 AM intensity (data not shown) and thus experiment could not proceed any further. However, our results strongly suggested that the mitochondrial Ca^{2+} release by $sA\beta_{1-42}$ plays an important role in cytosolic Ca^{2+} elevation and synapsin phosphorylation.

Although previous studies have showed that synaptic vesicles are shared constitutively between presynaptic terminals [24, 48], little is known about their functional roles and regulation mechanisms. One key aspect of vesicle sharing is its significant role in a variety of different forms of plasticity. We found that $sA\beta_{1-42}$ strongly inhibited activity-dependent rapid synaptogenesis, suggesting that inhibition of intersynaptic vesicle trafficking could be one of the cellular mechanisms underlying the $sA\beta_{1-42}$-induced defects in synaptic plasticity [49]. Conversely, this type of mechanism for allocating synaptic weights across multiple neighboring synapses could contribute to presynaptic homeostatic rescaling or balancing of SV pool size among synapses. In this study, we demonstrated that $sA\beta_{1-42}$ disrupted the regulatory mechanism of balancing SV pool sizes between presynaptic terminals by inhibiting intersynaptic vesicle sharing and thus increases the heterogeneity in SV pool size. In either case, the inhibition of intersynaptic trafficking caused by $sA\beta_{1-42}$ alters synaptic strength and efficacy, leading to the defects in synaptic plasticity and homeostatic regulation, which could contribute to synaptic dysfunctions observed in early AD.

Finally, although the in vitro system used in this study does not mimic the exact disease state that underlies AD, our results identify the novel $sA\beta_{1-42}$-induced defect in presynaptic function associated with the early stages of AD. Therefore, this work suggests a possible therapeutic target that prevents $sA\beta_{1-42}$-induced synaptic dysfunction in early-stage AD.

Methods

$sA\beta_{1-42}$ preparation and treatment

$sA\beta_{1-42}$ was prepared from synthetic $A\beta_{1-42}$ peptide (Bachem) as previously described [27, 50, 51]. Briefly, 1 mM HFIP (1,1,1,3,3,3-hexafluoro-2-propanol, Sigma) was added to dissolve synthetic $A\beta_{1-42}$ peptide and incubated at room temperature (RT) for 1 h. Then, HFIP was evaporated and dried from aliquots to make peptide film. Peptide film was dissolved in 1 mM dimethyl sulfoxide (DMSO) and Ham's F-12 (phenol red-free, ThermoFisher scientific) was added for dilution and incubated over 12 h at 4 °C for oligomerization. $sA\beta_{1-42}$ oligomer was confirmed by western-blot before experiments. Unless otherwise indicated, prepared $sA\beta_{1-42}$ was diluted with cultured neurobasal media to the final concentration of 200 nM and treated to neurons for 2 h. To eliminate the $sA\beta_{1-42}$ effects, diluted $sA\beta_{1-42}$ was preincubated with Aβ antibody, 6E10 (Covance) for 2 h before treatment.

Antibodies

Anti-bassoon (cat# ab82958, Abcam), anti-synaptophysin 1 (cat# 101011, Synaptic Systems), anti-phospho-S9-synapsin (cat# 2311, Cell Signaling Technology), anti-synapsin I (cat# 106103, Synaptic Systems), anti-phospho-Thr196-CaMKIV (cat# Sc-28,443-R, Santa Cruz Biotechnology), anti-CaMKIV (cat# ab3557, Abcam), anti-mCherry (cat# ab167453, Abcam), anti-actin (cat# A4700, Sigma) and 6E10 antibody (cat# SIG-39300, Covance) were used in the experiments.

Hippocampal neuron culture and transfection

Hippocampal neurons were derived from embryonic day 18 fetal Sprague-Dawley rats and transfected at day in vitro 8 (DIV8) as previously described [27]. Briefly, dissociated hippocampal neurons were plated on poly-D-lysine coated glass coverslips and grown in the neurobasal medium supplemented with 2% B-27 (ThermoFisher scientific), 0.5 mM L-glutamine (Gibco) and 4 μM cytosine-1-β-D-arabinofuranoside (Ara-C; Sigma). At DIV8, neurons were transfected using the modified Ca^{2+} phosphate method. Briefly, 6 μg of DNA and 9.3 μl of 2 M $CaCl_2$ were mixed in distilled water to a total volume of 75 μl, and the same volume of 2 × BBS [50 mM BES, 280 mM NaCl, and 1.5 mM Na_2HPO_4, pH 7.1] was added. The cell culture medium was completely replaced by transfection medium [minimum essential medium (MEM) 1 mM pyruvate, 0.6% glucose, 10 mM glutamine, and 10 mM HEPES, pH 7.65], and the DNA mixture was added to the cells and incubated in a 5% CO_2 incubator for 60 min. Cells were washed twice with washing medium (pH 7.35) and then returned to the original culture medium. All animal experiments were approved by the Institute of Animal Care and Use Committee of Seoul National University, Korea.

HEK293T cell transfection

HEK293T cells were transfected by Lipofectamine-2000 reagent (ThermoFisher scientific) following the manufacturer's instruction. Briefly, 3 μg of plasmid DNA were mixed with 6 μl of Lipofectamine-2000 in the 200 μl of Opti-MEM solution (ThermoFisher scientific) followed by 20 min incubation at RT. Then, mixture was treated to HEK293T cells (60~ 70% confluency) in serum-free

medium (Dulbecco's Modified Eagle's Medium, DMEM) for 3 h and the medium was replaced by complete medium (DMEM with 10% FBS). After 48 h, the cells were lysed for western blot.

Immunocytochemistry

Cultured neurons were fixed in 4% paraformaldehyde in 4% sucrose/PBS for 15 min at RT and permeabilized with 0.25% triton X-100 solution for 5 min at RT. After permeabilization, neurons were blocked with 10% BSA/PBS for 30 min at RT. Then, neurons were incubated with primary antibody in 3% BSA/PBS for 2 h at RT and with Alexa Fluor conjugated secondary antibody in 3% BSA/PBS for 45 min at RT.

FRAP assay

Cultured hippocampal neurons were transfected with GFP-synapsin and fluorescence recovery after photobleaching (FRAP) assay was performed on a Fluoview-1000 confocal microscope (Olympus) with a 100 x, 1.4 N.A. objective lens. Neurons were incubated in pre-warmed tyrode solution [136 mM NaCl, 2.5 mM KCl, 2 mM $CaCl_2$, 1.3 mM $MgCl_2$, 10 mM HEPES and 10 mM glucose], and single bouton was bleached to 50% of the original fluorescence intensity by scanning with a 488 nm laser at 50% of total laser power for 2 s. Time-lapse images were acquired every 5 s for 150 s and analyzed by using Olympus Fluoview software and OriginPro 9.0 (OriginLab).

Synaptic vesicle tracking and analysis

GFP-synaptophysin expressing neurons were time-lapse imaged for 1 min with 0.5 s intervals to track the synaptic vesicle movements. Each x and y coordination of synaptic vesicles in time-lapse images was acquired using MetaMorph software (Molecular Devices) and the mean square displacement (MSD) was calculated using formula below [27, 52].

$$\mathrm{MSD}(n\tau) = \frac{1}{N-n}\sum_{i=1}^{N-n}\left[(x((i+n)\tau)-x(i\tau))^2 + (y((i+n)\tau)-y(i\tau))^2\right]$$

xi and yi are coordinates of synaptic vesicle, N is the total number of steps in the trajectory and τ is the acquisition time. First five points of the MSD versus time were linear-fitted and the diffusion coefficient was calculated using the equation $\mathrm{MSD}(n\tau) \approx 4Dn\tau$.

Image acquisition and data analysis

Time-lapse images were acquired with an Olympus IX-71 inverted microscope (Olympus) with 40 x oil lens (1.0 N.A.) using an Andor iXon 897 EMCCD camera (Andor Technologies) and Touchbright LED light source (LCI) controlled by MetaMorph software. Tyrode solution included 10 μM 6-cyano-7-nitroquinoxaline-2,3-dione to prevent any recurrent excitation. Analysis and quantification of data were performed with MetaMorph software, ImageJ (NIH) and OriginPro 9.0 in a double- blind manner to avoid experimenter bias. Statistical comparisons were performed with Origin 9.0 and SPSS (IBM) software. Student's t test was performed for comparisons between two independent groups. For multiple group comparison, one-way ANOVA followed by Tukey's post hoc test was performed.

Ca^{2+} measurements

To detect the Ca^{2+} dynamics, cultured neurons were incubated with 0.5 μM Fluo-4 AM Ca^{2+} indicator (F14201, ThermoFisher scientific) for 15 min at 37 °C. After 10 min of wash-out in tyrode, Fluo-4 AM intensity was measured before and after 5 min treatment of $sA\beta_{1-42}$. To see the blockage effect of TPP (Sigma), Fluo-4 AM loaded neurons were pre-incubated with extracellular buffer as indicated (normal tyrode (2 mM Ca^{2+}), Ca^{2+}-free tyrode containing EDTA, normal tyrode containing 2 μM TPP, Ca^{2+}-free tyrode containing EDTA and 2 μM TPP) for 5 min and the changes in Fluo-4 AM intensity after $sA\beta_{1-42}$ or TPP treatment were measured by time-lapse imaging (5 s intervals). To confirm the levels of synapsin phosphorylation induced by $sA\beta_{1-42}$ in 0 mM extracellular Ca^{2+}, neurons were each treated with DMSO, 2 μM TPP, 200 nM $sA\beta_{1-42}$, or 200 nM $sA\beta_{1-42}$ with 2 μM TPP for 2 h in Ca^{2+}-free tyrode containing EDTA. After then, neuron lysates from each treatment group were western blotted to measure the level of phospho- and total-synapsin I.

Immunoprecipitation

Transfected HEK293T cells were lysed in a 1% triton X-100 lysis buffer [20 mM Tris-HCl, pH 8, 1% triton X-100, 10% glycerol, 137 mM NaCl, 2 mM EDTA] with 1% seine/threonine phosphatase inhibitor (Sigma) and protease inhibitor cocktail (Sigma). After sonication and centrifugation, anti-synapsin I antibody (Synaptic Systems) was added to each of equal amounts of total cell lysate (500 μg). The samples were incubated overnight at 4 °C, then 30 μl Protein A-Sepharose (GE healthcare) was added and incubated for 1 h at 4 °C. The samples were washed three times with lysis buffer and then bead pellets were eluted with 30 μl of 2× sample buffer [100 mM Tris-HCl (pH 6.8), 4% sodium dodecyl sulfate, 0.2% bromophenol blue, 20% glycerol and 2% beta-mercaptoethanol] followed by boiling (100 °C, 5 min) and gel loading.

Western blot

Cultured rat hippocampal neurons at DIV14–16 were lysed with 1% triton X-100 lysis buffer with 1% seine/threonine phosphatase inhibitor (Sigma) and protease inhibitor cocktail (Sigma). Lysates were centrifuged at

14,000 g at 4 °C for 20 min after sonication. Supernatants were collected and protein concentration was measured using BCA assay kit. Equal amounts of protein were loaded on to polyacrylamide gels. Gels were transferred to PVDF membranes (Pall Life Sciences, Ann Arbor, MI), then the membranes were incubated with 10% BSA/PBS or 5% SKIM milk/PBS for 30 min at RT. After washing in TBST, PVDF membranes were incubated with the primary antibody for overnight at 4 °C, followed by the horseradish peroxidase (HRP)-conjugated secondary antibody (Jackson ImmunoResearch Laboratories, West Grove, PA) for 1 h at RT. ECL solution (AbClon) and LAS 4000 (GE healthcare) were used to detect immunoreaction. Band intensities were calculated using imageJ.

Additional file

Additional file 1: Figure S1. Phospho-deficient mutants of synapsin serine 9 (S9A) residue and actin binding. (**a**) Representative western blot images for immunoprecipitation and total cell lysate. (**b**) Quantitative analysis from 4 independent blots (1±0 for control, 1.94±0.27 for S9A). Values are means±SEM. N.S = no significant difference, * $p < 0.05$ (Student's *t*-test). (PDF 345 kb)

Abbreviations

A. F. U: Arbiturary fluorescence unit; AD: Alzheimer's disease; Aβ: Amyloid beta; Ca^{2+}: Calcium; CaMKIV: Ca^{2+}/calmodulin-dependent protein kinases IV; Diffusion Coeffi: Diffusion coefficient; DIV: Day in vitro; F: Fluorescence; FCCP: Carbonyl cyanide p-(trifluoromethoxy)-phenylhydrazone; FRAP: Fluorescence recovery after photobleaching; IB: Immuno blot; MSD: Mean square displacement; P-Syn: Phospho-synapsin; RT: Room temperature; $sA\beta_{1-42}$: Prefibrillar form of soluble $A\beta_{1-42}$; SV: Synaptic vesicle; Syn: Synapsin; TPP: Tetraphenylphosphonium; VDCC: Voltage dependent calcium channel; WT: Wild type

Acknowledgements

We are grateful to the Biomedical Imaging Center at the Seoul National University College of Medicine for the microscope services.

Funding

This research was supported by grants from the Brain Research Program (NRF-2017M3C7A1044957–8 and 2015M3C7A1028790) to SC through the National Research Foundation of Korea funded by the Ministry of Science, ICT & Future Planning, Republic of Korea. This work was also supported by the Education and Research Encouragement Fund of Seoul National University Hospital.

Availability of data and materials

The datasets used and/or analyzed during the current study are available from the corresponding author on reasonable request.

Authors' contributions

DP and SC designed the experiments. DP performed the experiments. DP and SC analyzed the data and DP. SC. wrote the paper. Both authors read and approved the final manuscript.

Ethics approval

All of animal experiments were performed in accordance with the guidelines set by Institute of Animal Care and Use Committee (IACUC) of Seoul National University, Korea.

Consent for publication

Not applicable.

Competing interests

The authors declare that they have no competing interests.

Publisher's Note

Received: 30 January 2018 Accepted: 13 February 2018
Published online: 20 February 2018

References

1. Walsh DM, Klyubin I, Fadeeva JV, Cullen WK, Anwyl R, Wolfe MS, Rowan MJ, Selkoe DJ. Naturally secreted oligomers of amyloid beta protein potently inhibit hippocampal long-term potentiation in vivo. Nature. 2002;416(6880):535–9.
2. McLean CA, Cherny RA, Fraser FW, Fuller SJ, Smith MJ, Beyreuther K, Bush AI, Masters CL. Soluble pool of Abeta amyloid as a determinant of severity of neurodegeneration in Alzheimer's disease. Ann Neurol. 1999;46(6):860–6.
3. Haass C, Selkoe DJ. Soluble protein oligomers in neurodegeneration: lessons from the Alzheimer's amyloid beta-peptide. Nat Rev Mol Cell Biol. 2007;8(2):101–12.
4. Selkoe DJ. Alzheimer's disease is a synaptic failure. Science. 2002;298(5594):789–91.
5. Benilova I, Karran E, De Strooper B. The toxic Abeta oligomer and Alzheimer's disease: an emperor in need of clothes. Nat Neurosci. 2012;15(3):349–57.
6. Berridge MJ. Calcium regulation of neural rhythms, memory and Alzheimer's disease. J Physiol. 2014;592(2):281–93.
7. Demuro A, Parker I, Stutzmann GE. Calcium signaling and amyloid toxicity in Alzheimer disease. J Biol Chem. 2010;285(17):12463–8.
8. Stutzmann GE, Mattson MP. Endoplasmic reticulum ca(2+) handling in excitable cells in health and disease. Pharmacol Rev. 2011;63(3):700–27.
9. Koh SH, Noh MY, Kim SH. Amyloid-beta-induced neurotoxicity is reduced by inhibition of glycogen synthase kinase-3. Brain Res. 2008;1188:254–62.
10. Ma QL, Yang F, Rosario ER, Ubeda OJ, Beech W, Gant DJ, Chen PP, Hudspeth B, Chen C, Zhao Y, et al. Beta-amyloid oligomers induce phosphorylation of tau and inactivation of insulin receptor substrate via c-Jun N-terminal kinase signaling: suppression by omega-3 fatty acids and curcumin. J Neurosci. 2009;29(28):9078–89.
11. Mairet-Coello G, Courchet J, Pieraut S, Courchet V, Maximov A, Polleux F. The CAMKK2-AMPK kinase pathway mediates the synaptotoxic effects of Abeta oligomers through tau phosphorylation. Neuron. 2013;78(1):94–108.
12. Henriques AG, Vieira SI, da Cruz ESEF, da Cruz ESOA. Abeta promotes Alzheimer's disease-like cytoskeleton abnormalities with consequences to APP processing in neurons. J Neurochem. 2010;113(3):761–71.
13. Calkins MJ, Reddy PH. Amyloid beta impairs mitochondrial anterograde transport and degenerates synapses in Alzheimer's disease neurons. Biochim Biophys Acta. 2011;1812(4):507–13.
14. Manelli AM, Bulfinch LC, Sullivan PM, LaDu MJ. Abeta42 neurotoxicity in primary co-cultures: effect of apoE isoform and Abeta conformation. Neurobiol Aging. 2007;28(8):1139–47.
15. Hsieh H, Boehm J, Sato C, Iwatsubo T, Tomita T, Sisodia S, Malinow R. AMPAR removal underlies Abeta-induced synaptic depression and dendritic spine loss. Neuron. 2006;52(5):831–43.
16. Palop JJ, Mucke L. Amyloid-beta-induced neuronal dysfunction in Alzheimer's disease: from synapses toward neural networks. Nat Neurosci. 2010;13(7):812–8.
17. Shankar GM, Bloodgood BL, Townsend M, Walsh DM, Selkoe DJ, Sabatini BL. Natural oligomers of the Alzheimer amyloid-beta protein induce reversible synapse loss by modulating an NMDA-type glutamate receptor-dependent signaling pathway. J Neurosci. 2007;27(11):2866–75.
18. Abramov E, Dolev I, Fogel H, Ciccotosto GD, Ruff E, Slutsky I. Amyloid-beta as a positive endogenous regulator of release probability at hippocampal synapses. Nat Neurosci. 2009;12(12):1567–76.
19. Calabrese B, Shaked GM, Tabarean IV, Braga J, Koo EH, Halpain S. Rapid, concurrent alterations in pre- and postsynaptic structure induced by naturally-secreted amyloid-beta protein. Mol Cell Neurosci. 2007;35(2):183–93.
20. Moreno H, Yu E, Pigino G, Hernandez AI, Kim N, Moreira JE, Sugimori M, Llinas RR. Synaptic transmission block by presynaptic injection of oligomeric amyloid beta. Proc Natl Acad Sci U S A. 2009;106(14):5901–6.
21. Nimmrich V, Grimm C, Draguhn A, Barghorn S, Lehmann A, Schoemaker H, Hillen H, Gross G, Ebert U, Bruehl C. Amyloid beta oligomers (a beta(1-42) globulomer) suppress spontaneous synaptic activity by inhibition of P/Q-type calcium currents. J Neurosci. 2008;28(4):788–97.

22. Puzzo D, Privitera L, Leznik E, Fa M, Staniszewski A, Palmeri A, Arancio O. Picomolar amyloid-beta positively modulates synaptic plasticity and memory in hippocampus. J Neurosci. 2008;28(53):14537–45.
23. Park J, Jang M, Chang S. Deleterious effects of soluble amyloid-beta oligomers on multiple steps of synaptic vesicle trafficking. Neurobiol Dis. 2013;55:129–39.
24. Darcy KJ, Staras K, Collinson LM, Goda Y. Constitutive sharing of recycling synaptic vesicles between presynaptic boutons. Nat Neurosci. 2006;9(3):315–21.
25. Krueger S, Fitzsimonds RM. Remodeling the plasticity debate: the presynaptic locus revisited. Physiology (Bethesda). 2006;21:346–51.
26. Staras K. Share and share alike: trading of presynaptic elements between central synapses. Trends Neurosci. 2007;30(6):292–8.
27. Park D, Na M, Kim JA, Lee U, Cho E, Jang M, Chang S. Activation of CaMKIV by soluble amyloid-beta1-42 impedes trafficking of axonal vesicles and impairs activity-dependent synaptogenesis. Sci Signal. 2017;10(487):1-11.
28. Moreira PI, Carvalho C, Zhu X, Smith MA, Perry G. Mitochondrial dysfunction is a trigger of Alzheimer's disease pathophysiology. Biochim Biophys Acta. 2010;1802(1):2–10.
29. Deryabina YI, Bazhenova EN, Saris NE, Zvyagilskaya RA. Ca(2+) efflux in mitochondria from the yeast Endomyces magnusii. J Biol Chem. 2001; 276(51):47801–6.
30. Orenbuch A, Shalev L, Marra V, Sinai I, Lavy Y, Kahn J, Burden JJ, Staras K, Gitler D. Synapsin selectively controls the mobility of resting pool vesicles at hippocampal terminals. J Neurosci. 2012;32(12):3969–80.
31. Krueger SR, Kolar A, Fitzsimonds RM. The presynaptic release apparatus is functional in the absence of dendritic contact and highly mobile within isolated axons. Neuron. 2003;40(5):945–57.
32. Hoopmann P, Punge A, Barysch SV, Westphal V, Buckers J, Opazo F, Bethani I, Lauterbach MA, Hell SW, Rizzoli SO. Endosomal sorting of readily releasable synaptic vesicles. Proc Natl Acad Sci U S A. 2010;107(44):19055–60.
33. Di Giovanni J, Sheng ZH. Regulation of synaptic activity by snapin-mediated endolysosomal transport and sorting. EMBO J. 2015;34(15):2059–77.
34. Cirnaru MD, Marte A, Belluzzi E, Russo I, Gabrielli M, Longo F, Arcuri L, Murru L, Bubacco L, Matteoli M, et al. LRRK2 kinase activity regulates synaptic vesicle trafficking and neurotransmitter release through modulation of LRRK2 macro-molecular complex. Front Mol Neurosci. 2014;7:49.
35. Lei M, Xu H, Li Z, Wang Z, O'Malley TT, Zhang D, Walsh DM, Xu P, Selkoe DJ, Li S. Soluble Abeta oligomers impair hippocampal LTP by disrupting glutamatergic/GABAergic balance. Neurobiol Dis. 2016;85:111–21.
36. Li S, Hong S, Shepardson NE, Walsh DM, Shankar GM, Selkoe D. Soluble oligomers of amyloid Beta protein facilitate hippocampal long-term depression by disrupting neuronal glutamate uptake. Neuron. 2009;62(6):788–801.
37. Green KN, LaFerla FM. Linking calcium to Abeta and Alzheimer's disease. Neuron. 2008;59(2):190–4.
38. Ferreiro E, Oliveira CR, Pereira CM. The release of calcium from the endoplasmic reticulum induced by amyloid-beta and prion peptides activates the mitochondrial apoptotic pathway. Neurobiol Dis. 2008; 30(3):331–42.
39. Arispe N, Rojas E, Pollard HB. Alzheimer disease amyloid beta protein forms calcium channels in bilayer membranes: blockade by tromethamine and aluminum. Proc Natl Acad Sci U S A. 1993;90(2):567–71.
40. Luo Y, Bond JD, Ingram VM. Compromised mitochondrial function leads to increased cytosolic calcium and to activation of MAP kinases. Proc Natl Acad Sci U S A. 1997;94(18):9705–10.
41. Martin SW, Butcher AJ, Berrow NS, Richards MW, Paddon RE, Turner DJ, Dolphin AC, Sihra TS, Fitzgerald EM. Phosphorylation sites on calcium channel alpha1 and beta subunits regulate ERK-dependent modulation of neuronal N-type calcium channels. Cell Calcium. 2006;39(3):275–92.
42. Fitzgerald EM. Regulation of voltage-dependent calcium channels in rat sensory neurones involves a Ras-mitogen-activated protein kinase pathway. J Physiol. 2000;527(Pt 3):433–44.
43. Brocard JB, Tassetto M, Reynolds IJ. Quantitative evaluation of mitochondrial calcium content in rat cortical neurones following a glutamate stimulus. J Physiol. 2001;531(Pt 3):793–805.
44. Gunter TE, Wingrove DE, Banerjee S, Gunter KK. Mechanisms of mitochondrial calcium transport. Adv Exp Med Biol. 1988;232:1–14.
45. Jensen JR, Rehder V. FCCP releases Ca2+ from a non-mitochondrial store in an identified Helisoma neuron. Brain Res. 1991;551(1–2):311–4.
46. Raffaello A, Mammucari C, Gherardi G, Rizzuto R. Calcium at the Center of Cell Signaling: interplay between endoplasmic reticulum, mitochondria, and lysosomes. Trends Biochem Sci. 2016;41(12):1035–49.
47. Arispe N, Pollard HB, Rojas E. Zn2+ interaction with Alzheimer amyloid beta protein calcium channels. Proc Natl Acad Sci U S A. 1996;93(4):1710–5.
48. Staras K, Branco T, Burden JJ, Pozo K, Darcy K, Marra V, Ratnayaka A, Goda Y. A vesicle superpool spans multiple presynaptic terminals in hippocampal neurons. Neuron. 2010;66(1):37–44.
49. Ma T, Klann E. Amyloid beta: linking synaptic plasticity failure to memory disruption in Alzheimer's disease. J Neurochem. 2012;120(Suppl 1):140–8.
50. Berman DE, Dall'Armi C, Voronov SV, McIntire LB, Zhang H, Moore AZ, Staniszewski A, Arancio O, Kim TW, Di Paolo G. Oligomeric amyloid-beta peptide disrupts phosphatidylinositol-4,5-bisphosphate metabolism. Nat Neurosci. 2008;11(5):547–54.
51. Dahlgren KN, Manelli AM, Stine WB Jr, Baker LK, Krafft GA, LaDu MJ. Oligomeric and fibrillar species of amyloid-beta peptides differentially affect neuronal viability. J Biol Chem. 2002;277(35):32046–53.
52. Lee S, Jung KJ, Jung HS, Chang S. Dynamics of multiple trafficking behaviors of individual synaptic vesicles revealed by quantum-dot based presynaptic probe. PLoS One. 2012;7(5):e38045.